THE JOURNAL OF BIOLOGICAL CHEMISTRY VOL. 287, NO. 47, pp. 39911–39924, November 16, 2012

PACSIN1, a Tau-interacting Protein, Regulates Axonal Elongation and Branching by Facilitating Microtubule Instability*[S]

Received for publication, July 21, 2012, and in revised form, September 26, 2012 Published, JBC Papers in Press, October 3, 2012, DOI 10.1074/jbc.M112.403451

Yingying Liu[‡1], **Kaosheng Lv**[‡1], **Zenglong Li**[‡], **Albert C. H. Yu**[§], **Jianguo Chen**[‡¶2], **and Junlin Teng**[‡3]

From the [‡]*Key Laboratory of Cell Proliferation and Differentiation of the Ministry of Education and State Key Laboratory of Bio-membrane and Membrane Bio-engineering, College of Life Sciences, and* [¶]*Center for Theoretical Biology, Peking University, Beijing 100871 and the* [§]*Neuroscience Research Institute, Department of Neurobiology, School of Basic Medical Sciences, Key Laboratory for Neuroscience (Ministry of Education and Ministry of Public Health), Peking University, Beijing 100191, China*

Background: The regulation of microtubule dynamics is crucial for forming and maintaining neuronal polarity.
Results: PACSIN1 interacts with Tau in axons and reduces axonal elongation and branching by promoting microtubule dynamics.
Conclusion: PACSIN1 acts as a Tau-binding partner in regulating microtubule dynamics and is required for axonal plasticity.
Significance: Learning how PACSIN1 regulates microtubule dynamics is important for understanding its roles in neuronal development and nervous system disorders.

Tau is a major member of the neuronal microtubule-associated proteins. It promotes tubulin assembly and stabilizes axonal microtubules. Previous studies have demonstrated that Tau forms cross-bridges between microtubules, with some particles located on cross-bridges, suggesting that some proteins interact with Tau and might be involved in regulating Tau-related microtubule dynamics. This study reports that PACSIN1 interacts with Tau in axon. PACSIN1 blockade results in impaired axonal elongation and a higher number of primary axonal branches in mouse dorsal root ganglia neurons, which is induced by increasing the binding ability of Tau to microtubules. In PACSIN1-blocked dorsal root ganglia neurons, a greater amount of Tau is inclined to accumulate in the central domain of growth cones, and it promotes the stability of the microtubule network. Taken together, these results suggest that PACSIN1 is an important Tau binding partner in regulating microtubule dynamics and forming axonal plasticity.

The regulation of microtubule dynamics is crucial for forming and maintaining neuronal polarity (1–4). In polarized neurons, axonal microtubule organization is largely dependent on Tau, a microtubule-associated protein (MAP)[4] mainly concentrated in neuronal axons (5, 6). Tau forms cross-bridges and determines the distance between adjacent microtubules in axons (7), which promotes microtubule assembly, stabilization, and bundling (7–9). In small caliber axons in Tau-deficient mice, microtubule density and stability are decreased, despite compensation by MAP1A (10). Meanwhile, Tau and MAP1B have overlapping functions in axonal elongation and neuronal migration, because $tau^{-/-}map1b^{-/-}$ double knock-out mice exhibit significantly more severe defects than single knock-out mice (11). In addition, a host of kinases, including GSK-3β and microtubule affinity-regulating kinase, reduce Tau affinity to microtubules and contribute to microtubule plasticity needed for neuronal polarity (12–14). However, pathological hyperphosphorylation of Tau results in detached Tau from microtubules and aggregates into paired-helical filaments in Alzheimer disease (15).

PACSIN1 (also known as SYNDAPIN1) is a neuron-specific member of the PACSIN family, which contains a highly conserved SH3 and F-BAR domain (16). PACSIN1 was originally identified as a molecular link between membrane trafficking and actin organization (17). It interacts with vesicle-associated proteins, including large GTPase DYNAMIN I and EHD proteins, and it plays an important role in endocytosis and endosomal recycling (18–20). In addition, it forms a complex with the Arp2/3 complex activator N-WASP and induces actin rearrangement (21, 22). Moreover, PACSIN1 interacts with tubulin and is involved in microtubule nucleation (23). Recently, the F-BAR domain of PACSIN1 was reported to regulate membrane deformation and shaping of the neuronal plasma membrane (24, 25).

This study hypothesized that Tau-binding proteins exist, because the quick-freeze, deep-etch electron microscopy technique identified particles on Tau-formed cross-bridges between microtubules (7). PACSIN1 was identified as a Tau-binding partner. This interaction was characterized to reduce Tau-binding affinity to microtubules and suppress Tau-induced microtubule polymerization/stability/bundling. Through the use of a

* This work was supported by the National Natural Science Foundation of China Grants 30670659 and 31071177 and Major State Basic Research Development Program of China (973 Program) Grant 2010CB833705.
[S] This article contains supplemental Figs. 1–3 and Movies 1 and 2.
[1] Both authors contributed equally to this work.
[2] To whom correspondence may be addressed. Tel.: 86-10-62755786; Fax: 86-10-62755786; E-mail: chenjg@pku.edu.cn.
[3] To whom correspondence may be addressed. Tel.: 86-10-62767044; Fax: 86-10-62755786; E-mail: junlinteng@pku.edu.cn.
[4] The abbreviations used are: MAP, microtubule-associated protein; MBD, microtubule binding domain; PRD, proline-rich domain; DRG, dorsal root ganglia; GC, growth cone; C domain, central domain; P domain, peripheral domain; Ab, antibody; PFA, paraformaldehyde; DIV, days *in vitro*; SH3, Src homology 3; RFP, red fluorescent protein.

model system of cultured dorsal root ganglia (DRG) neurons, PACSIN1 blocking resulted in a greater number of straight/spread microtubules via altered Tau distribution in growth cones (GCs), as well as decreased axonal length with a higher number of primary axonal branches. These phenotypes were partially abolished by functional inhibition of PACSIN1 and Tau. These results shed new light on the function of PACSIN1 and the regulation of microtubule dynamics and proper axonal morphogenesis.

EXPERIMENTAL PROCEDURES

cDNA Construction—Full-length PACSIN1 cDNA (a gift from Dr. Markus Plomann) (16) was subcloned into the BglII site on pEGFP-C1 (Clontech) and the EcoRI/XhoI sites on pCMV-Tag5A (Stratagene). Mutant PACSIN1 P434L was subcloned into the EcoRI/XhoI sites on pCMV-Tag5A. The Tau isoform L4 (TauL4) (26) was inserted into the BglII/EcoRI sites on pEGFP-C1 and pEmRFP-C1 (replace GFP sequence with monomer RFP sequence on pEGFP-C1).

Antibodies—For PACSIN1 and Tau antibody production, full-length PACSIN1 and microtubule binding domain (MBD) deletion mutant of TauL4 (TauL4ΔMBD) were cloned into the expression vector pGEX-4T-1 (EcoRI/XhoI and EcoRI/SalI sites, respectively). GST-PACSIN1 and GST-TauL4ΔMBD fusion proteins were induced in *Escherichia coli* BL21. Fusion proteins were purified by affinity chromatography on glutathione-Sepharose 4B beads (GE Healthcare) and utilized as antigens to immunize rabbits and mice. Other antibodies were as follows: anti-α-Tubulin (DM1α, Sigma); anti-Tau (Tau-1, Roche Applied Science); anti-Neurofilament-L (clone DA2, Abcam, United Kingdom).

RNA Interference—RNAi constructs against mouse PACSIN1 and Tau were generated using pSuper vector (BglII/HindIII). The oligonucleotides are as follows: PACSIN1, 5′-GCGCCAGCTCATCGAGAAATTCAAGAGATTTCTCGATGAGCTGGCGC-3′ (27). Tau, 5′-GCAGTGTGCAAATAGTCTACATTCAAGAGATGTAGACTATTTGCACACTGC-3′.

Transient transfection of pEGFP-C1-PACSIN1 or pEGFP-C1-TauL4 together with interference plasmids into 293T cells was performed, and the effects of interference vectors were examined 72 h after transfection. In addition, DRG neurons were injected with interference vectors and pEGFP-C1 (concentration ratio = 3:1) at 5–12 h after plating. After 3 days, the injected DRG neurons were fixed for further analysis. The empty pSuper vector was used as negative control. pEGFP-C1 was co-injected with the interference plasmid to mark the injected neurons.

Pulldown Analysis and Protein Identification—The fusion protein GST-TauL4ΔMBD was incubated with glutathione-Sepharose 4B beads to establish an affinity column for pulldown experiments. Adult mouse brains were homogenized in lysis buffer (20 mM HEPES, pH 7.4, 1% Triton X-100) containing a protease inhibitor mixture (Roche Applied Science). The centrifuged homogenate was incubated with the affinity column. After washing with lysis buffer, the column was eluted with high salt buffers by stepwise increases in NaCl concentration (200, 400, 600, and 800 mM). The eluates were sequentially collected.

To identify proteins separated on SDS-polyacrylamide gels, bands were excised and digested with sequence grade-modified trypsin (Promega). The prepared samples were subjected to liquid chromatography/mass spectrometry with an LCQ Deca XP Plus Analyzer (Finnigan).

Immunoprecipitation—Cells overexpressing GFP-PACSIN1 and RFP-TauL4 were washed three times with PBS and lysed in lysis buffer (50 mM Tris, pH 7.5, 1 mM EDTA, 150 mM NaCl, 0.1% SDS, 1% Triton X-100, 10 mM NaF). The protease inhibitors aprotinin, pepstatin, leupeptin, and phenylmethanesulfonyl fluoride were added to this buffer before cell lysis. The lysates were centrifuged at 20,000 × *g* for 10 min two times. The supernatant was mixed with 10 μl of rabbit preimmune serum or rabbit anti-Tau or -PACSIN1 antibody and incubated at 4 °C overnight. Subsequently, 50 μl of protein A-Sepharose beads (Amersham Biosciences) were added, and the mixtures were rotated for 2 h at 4 °C. After washing extensively with lysis buffer, the bound immunocomplexes were eluted by boiling in loading buffer. The protein complexes were subjected to Western blot analysis as described previously (28), and then detected by anti-Tau (Tau-1) or anti-PACSIN1 mouse antibody.

Yeast Two-hybrid Assay—The protein interaction was examined using the Matchmaker Two-hybrid System 3 (Clontech). Full-length PACSIN1 and TauL4ΔMBD were separately cloned into pGADT7 and pGBKT7. The plasmids were co-transformed into the yeast strain AH109. Positive interactions were identified by growth on SD/−Trp/−His/−Leu/−Ade quadruple drop-out plates and the β-galactosidase assay.

Cell Culture, Transfection or Microinjection, Fixation, and Extraction—HeLa cells were seeded in DMEM (Invitrogen) with 10% fetal bovine serum in 5% CO_2 overnight and transfected with jetPEI (Polyplus transfection, France) for 24 h. Following transfection, cells were simultaneously fixed and permeabilized for 3 min at 37 °C using 2% paraformaldehyde (PFA) with 0.2% Triton X-100 in PEM buffer (80 mM PIPES, 1 mM $MgCl_2$, 1 mM EGTA, pH 6.8) containing 30% glycerol and then fixed at 37 °C with 4% PFA for 15 min. For repolymerization, cells were treated on ice for 2 h and incubated at 37 °C for various lengths of time to repolymerize. For nocodazole treatment, cells were treated with nocodazole (10 μg/ml) for 1.5 h.

Neuronal cultures were prepared as described (11, 29). To observe endogenous protein distribution, cultured hippocampal neurons were fixed without extraction with 4% PFA or fixed and permeabilized simultaneously (see HeLa cells experiment), and DRG neurons were fixed with 0.3% glutaraldehyde for 15 min in PEM buffer, with or without 0.5% Triton X-100, and quenched with $NaBH_4$ (30).

DRG neurons (cell body diameter >25 μm) were injected with specific antibody or nonspecific IgG (4 mg/ml) (all were rabbit polyclonal antibodies) at 5–12 h after plating. Anti-PACSIN1 and anti-Tau antibody were purified by ammonium sulfate precipitation. Nonspecific IgG was from Santa Cruz Biotechnology. The cells were then incubated for an additional 12–18 h in the presence of 100 ng/ml nerve growth factor (Invitrogen) prior to fixation for analysis. The injected cells were confirmed as DRG neurons by staining for Neurofilament-L, a neuronal marker protein.

Cryosections—Mice (1, 2, and 8 weeks old) were perfused with 4% PFA. Subsequently, the brains were resected, dehydrated, embedded, and sectioned as described previously (31). Cryosections were immunostained with anti-PACSIN1 and Tau antibodies and observed under a fluorescent microscope (TH4–200, Olympus).

Immunofluorescence—Immunostaining was performed using a previously described standard method (31). Briefly, after fixation, the cells were permeabilized with 0.2% Triton X-100 in PBS for 15 min. Following blocking with 5% BSA in PBS for at least 15 min, the cells were incubated with primary antibodies overnight at 4 °C. The secondary antibodies were Alexa Fluor 488-, 568-, and/or 633-conjugated goat anti-mouse and/or anti-rabbit IgG (Molecular Probes). The fixed and stained cells were observed under an LSM-510 confocal laser-scanning microscope (Zeiss), TCS SP2 confocal microscope (Leica), or IX71 inverted fluorescent microscope (Olympus). Live cell images were analyzed on an Andor Revolution XD laser confocal microscope system (Andor Technology). All above experiments were repeated 3–10 times with independent cellular preparations.

Electron Microscopy—Electron microscopy samples of injected neurons were prepared as described previously (31) and observed with a transmission electron microscope (JEOL, JEM 1010). The number of microtubules was estimated.

In Vitro Microtubule Assembly Assay—Mouse brain lysates were incubated with IgG or PACSIN1 Ab for 30 min at 35 °C in BRB80 buffer (80 mM PIPES, 1 mM EGTA, 1 mM $MgCl_2$, pH 6.8) containing 2 mM GTP. The mixtures were then centrifuged at 100,000 × *g* for 30 min. Supernatants and pellets were analyzed using SDS-PAGE and then detected by anti-Tau or anti-tubulin antibody.

Measurement and Statistical Analysis—Axonal lengths, fluorescence intensity (32), and band density from Western blot analysis were measured by ImageJ (National Institutes of Health) software or scion image (National Institutes of Health). Statistical methods from SPSS software are described in the figure legends.

RESULTS

PACSIN1 Directly Binds to the Proline-rich Domain (PRD) of Tau—To identify Tau-associated proteins involved in the regulation of Tau-related microtubule dynamics, the GST fusion protein was utilized in conjunction with a microtubule binding domain (MBD) deletion mutant of the Tau isoform L4 (GST-TauL4ΔMBD) (26), which does not bind to tubulin, as bait to pull down targets in adult mouse brain homogenates. The eluted samples were separated by SDS-PAGE and analyzed by mass spectrometry (supplemental Fig. 1, *A* and *B*). PACSIN1, which was eluted with 400 mM NaCl and had a molecular mass of ~50 kDa (supplemental Fig. 1*B*, *arrow*), was one of the interesting hits. We further confirmed that the identity of the 50-kDa band was PACSIN1 by immunoblotting in the GST-TauΔMBD pulldown complex (Fig. 1*A*). Reciprocally, Tau, but not MAP2, was also in the protein complex pulled down by GST-PACSIN1, suggesting the specific interaction between Tau and PACSIN1 (Fig. 1*B*). To confirm the biochemical interaction between Tau and PACSIN1, yeast two-hybrid assay was performed. Yeasts co-expressing TauL4ΔMBD and full-length PACSIN1 yielded a clear positive signal in the β-galactosidase assay, which suggested a direct interaction between the molecules (Fig. 1*C*).

To further analyze the Tau-binding region with PACSIN1, as well as TauL4ΔMBD, several GST fusion deletion mutants were constructed, including an MBD/PRD double deletion mutant (TauL4ΔMBDΔPRD) and PRD (TauL4-PRD) of Tau isoform L4 (Fig. 1*D*). After incubation of these recombinant mutants with His-PACSIN1, results showed that GST-TauL4-PRD bound to His-PACSIN1, but GST-TauL4ΔMBDΔPRD did not (Fig. 1*E*, *left panel*), indicating that Tau PRD was necessary and sufficient for the PACSIN1 interaction. PACSIN1 contains a CDC15 N-terminal (CDC15NT) domain, two asparagine-proline-phenylalanine (NPF), and an SH3 domain (18). Previous reports showed that the P434L mutation in the PACSIN1 SH3 domain impairs interaction with PRDs of its binding partners (17, 18). In this study, Tau interacted with PACSIN1 via PRD (Fig. 1*E*). Therefore, to determine whether PACSIN1 Pro-434 was important for Tau binding, a recombinant PACSIN1 mutant His-PACSIN1P434L was constructed. Binding of His-PACSIN1, but not His-PACSIN1P434L, with GST-TauL4ΔMBD and GST-TauL4PRD was revealed by Coomassie staining (Fig. 1*E*, *right panel*), indicating that Pro-434 was crucial for direct interaction between Tau and PACSIN1.

To further characterize the interaction between PACSIN1 and Tau, mouse and rabbit polyclonal anti-PACSIN1 and anti-Tau antibodies were generated using His-tagged full-length PACSIN1 and TauL4ΔMBD as antigens, respectively. Immunoblotting of adult mouse brain lysates with anti-PACSIN1 antibody recognized a specific band at a molecular mass of ~50 kDa (supplemental Fig. 2*A*). Analysis of PACSIN1 from several tissues showed that PACSIN1 was exclusively expressed in brain (supplemental Fig. 2*B*). Its expression increased continuously from embryonic day 14 (E14) to 4 weeks (supplemental Fig. 2*C*). These data are consistent with previous results (16). Immunoblotting of adult mouse brain lysates with anti-Tau antibody exhibited the same protein pattern with purchased monoclonal antibody Tau-1 (supplemental Fig. 2*D*). Subsequently, co-immunoprecipitation was performed to determine whether Tau and PACSIN1 form a complex within cells. In 293T cell lysates with overexpressing Tau and PACSIN1, anti-Tau antibodies immunoprecipitated Tau and PACSIN1. Reciprocally, Tau was present in protein complexes co-immunoprecipitated by anti-PACSIN1 antibody (Fig. 1*F*). In addition, endogenous Tau was co-immunoprecipitated in mouse brain lysates by anti-PACSIN1 antibody (Fig. 1*G*). These results suggested that PACSIN1 is a binding partner of Tau and forms complexes within cells.

Co-localization of PACSIN1 and Tau in Axons—Because PACSIN1 and Tau are neuronally specific proteins, their distribution in the brain was analyzed. In cryosections of the adult mouse brain, both PACSIN1 and Tau exhibited higher levels in corpus callosa and mossy fibers (supplemental Fig. 3). Co-localization of Tau and PACSIN1 in corpus callosa of 1- and 2-week-old mouse brains was also observed (data not shown). These results indicated Tau and PACSIN1 have a similar distribution pattern in the brain, especially in axonal fibers.

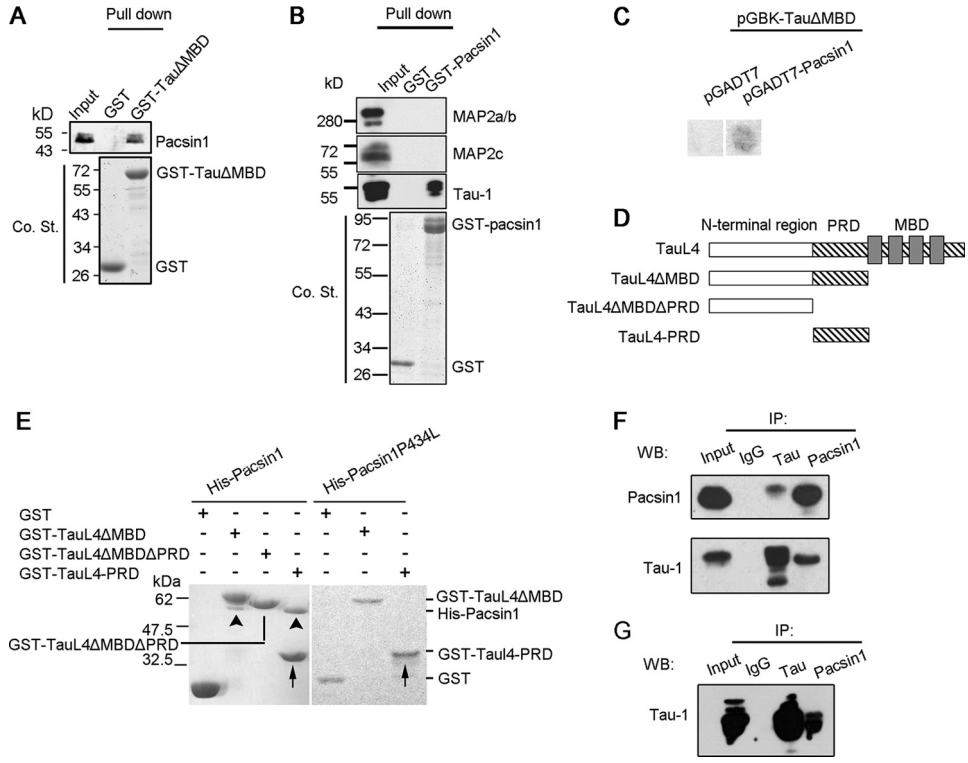

FIGURE 1. **Tau interacts with PACSIN1 through its PRD.** *A,* GST-TauΔMBD pulldown brain lysates. The pulldown complex was immunoblotted, and a 50-kDa band was recognized by PACSIN1 antibody. *Co. St*, Coomassie Blue staining. *B,* GST-PACSIN1 pulldown brain lysates. Tau, but not MAP2 isoforms, was present in PACSIN1 pulldown complex. *C,* interaction between Tau and PACSIN1 was tested in yeast by induction of reporter genes assayed via growth on quadruple drop-out plates and β-galactosidase activity. *D,* illustration of full-length TauL4 and deletion constructs used in this study. All deletion constructs carry an N-terminal GST tag. *E, in vitro* pulldown experiments demonstrated that GST-TauL4-PRD (*arrow*) is sufficient for interaction with His-PACSIN1. Neither GST alone nor GST-TauL4ΔMBDΔPRD interacts with PACSIN1 (*left panel*). His-PACSIN1 (*arrowheads*), but not His-PACSIN1P434L, interacts with GST-TauΔMBD and GST-Tau-PRD (*right panel*). *F,* TauL4 and PACSIN1 were co-immunoprecipitated from 293T cell lysates with ectopic TauL4 and PACSIN1. *G,* endogenous Tau was co-immunoprecipitated in mouse brain lysates by PACSIN1.

To determine subcellular localization, PACSIN1 and Tau distribution was analyzed in cultures of mouse hippocampal and DRG neurons. The strong PACSIN1 immunostaining signal was observed in both neurons. PACSIN1 exhibited discontinuous distribution (Fig. 2*A*, *upper panels*) and obvious puncta under higher magnification (Fig. 2*A*, *bottom panels*) in the neurites of hippocampal neurons at 9 days *in vitro* (DIV). The localization of PACSIN1 in DRG neurons was then analyzed, demonstrating enrichment in GCs and branch points (Fig. 2, *C* and *D, upper panels*). Tau distribution appeared to partially overlap with PACSIN1 in both neurons (Fig. 2, *A, C*, and *D, upper panels*). Because Tau is co-localized with detergent-resistant polymerized tubulin, neurons were permeabilized with Triton X-100 to further observe their localization in the cytoskeletal element. The enrichment of PACSIN1 decreased in GCs and branch points of DRG neurons as a result of permeabilization (Fig. 2, *C* and *D, bottom panels*), which demonstrated that most PACSIN1 was soluble. Following permeabilization, PACSIN1 and Tau staining exhibited weaker fluorescence and partially overlapped with each other in both neurons (Fig. 2, *B, C*, and *D, bottom panels*). These suggested that PACSIN1 and Tau are co-localized in the cytoskeleton network, as well as in the cytosol where they are in a soluble manner.

PACSIN1 Affects Axonal Growth and Branching via Tau Association—Based on the obvious co-localization of Tau and PACSIN1 in axons, the physiological function of this interaction in axonal morphogenesis was analyzed. Mouse DRG neuronal cultures serve as research material, because they are composed of only axons where PACSIN1 and Tau are co-localized, the larger cell size facilitates manipulation, and the extended GCs are easy to examine. To examine their interaction on axonal development, DRG neurons with single or double knockdown of PACSIN1 and Tau were established by microinjection of corresponding RNA interference constructs. These RNAi constructs successfully reduced the expression of PACSIN1 (by 70%) and Tau (by 80%), respectively (Fig. 3, *A–D*). The axonal length and number of primary branches of injected neurons were then examined at 3 DIV. PACSIN1-deficient neurons exhibited a shorter axonal length and higher number of primary branches (>10 μm) compared with control cells (Fig. 3, *E–G*). However, the effect of PACSIN1 deficiency was significantly alleviated when Tau and PACSIN1 were simultaneously deficient (Fig. 3, *E–G*), demonstrating Tau was indispensable for PACSIN1 effects on axonal growth and branching. These results suggested that PACSIN1 regulated axonal length and branching via Tau.

To confirm the phenotypes in RNAi experiments, PACSIN1 and Tau single- or double-blocked DRG neurons were established by microinjection of anti-PACSIN1 and/or anti-Tau antibodies (PACSIN1 Ab and/or Tau Ab). Following direct incubation with secondary antibodies, neurons injected with PACSIN1 Ab or Tau Ab exhibited an obvious PACSIN1 (dif-

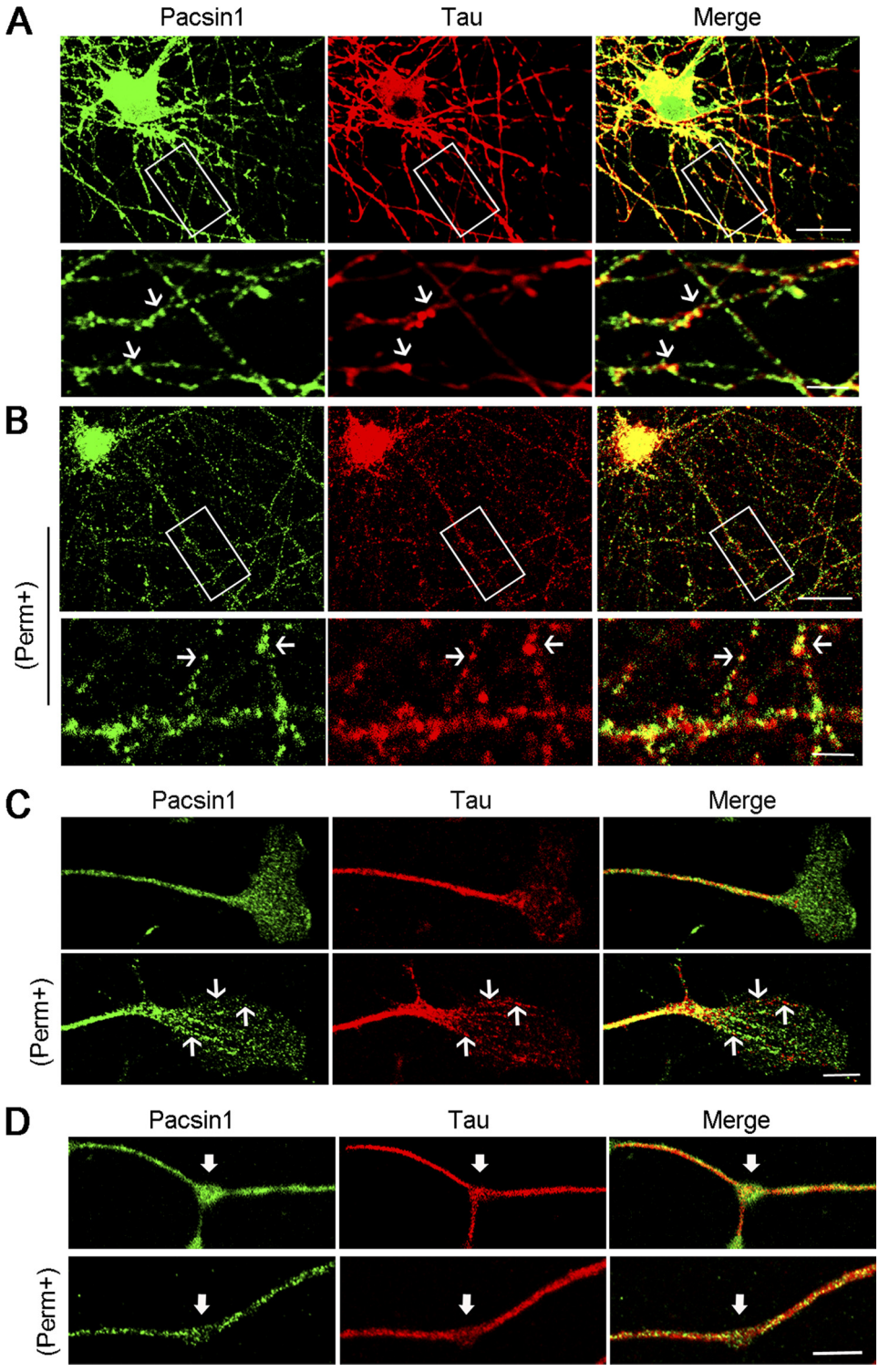

FIGURE 2. **Co-localization of PACSIN1 and Tau in axons.** *A* and *B,* co-localization of PACSIN1 and Tau in hippocampal neurons at 9 DIV. Nonpermeabilized neurons (*A*) or permeabilized neurons (*B*) were immunostained with anti-PACSIN1 (*green*) and anti-Tau (*red*) antibodies. *Bottom panels* are magnified view of the *boxed region* in *upper panels*. The *arrows* indicate co-localized puncta of PACSIN1 and Tau. *Scale bars, upper panels*, 20 μm; *bottom panels*, 5 μm. *C,* partial co-localization of PACSIN1 and Tau in GCs of DRG neurons. Neurons were fixed with (*bottom panels*) or without permeabilization (*upper panels*) and immunostained with anti-PACSIN1 (*green*) and anti-Tau (*red*) antibodies. The *arrows* indicate co-localized expression of PACSIN1 and Tau. *Scale bar,* 5 μm. *D,* immunofluorescent images of the axonal shaft of DRG neurons stained with anti-PACSIN1 (*green*) and anti-Tau (*red*) antibodies. Enrichment of PACSIN1 in branch points (*arrows, upper panels*). PACSIN1 enrichment disappeared after permeabilization (*bottom panels*). *Scale bar,* 5 μm.

fused and enriched in GC) or Tau distribution pattern (Fig. 4, *A* and *B*). These results indicated that the injected antibodies reacted with their antigens, respectively. The injected DRG neurons were examined at 1 DIV, and α-Tubulin was stained to visualize axonal length and primary branch number (>10 μm, positive for tubulin staining) (Fig. 4*C*). Blocking of PACSIN1 inhibited axonal elongation and promoted axonal branching of DRG neurons compared with control neurons injected with

IgG (Fig. 4, *D* and *E*). However, when the function of PACSIN1 and Tau was simultaneously blocked, the axonal length and branch number returned to control levels (Fig. 4, *D* and *E*). The results by antibody injection were consistent with those by RNAi, indicating that PACSIN1 Ab/Tau Ab could effectively block the function of PACSIN1/Tau.

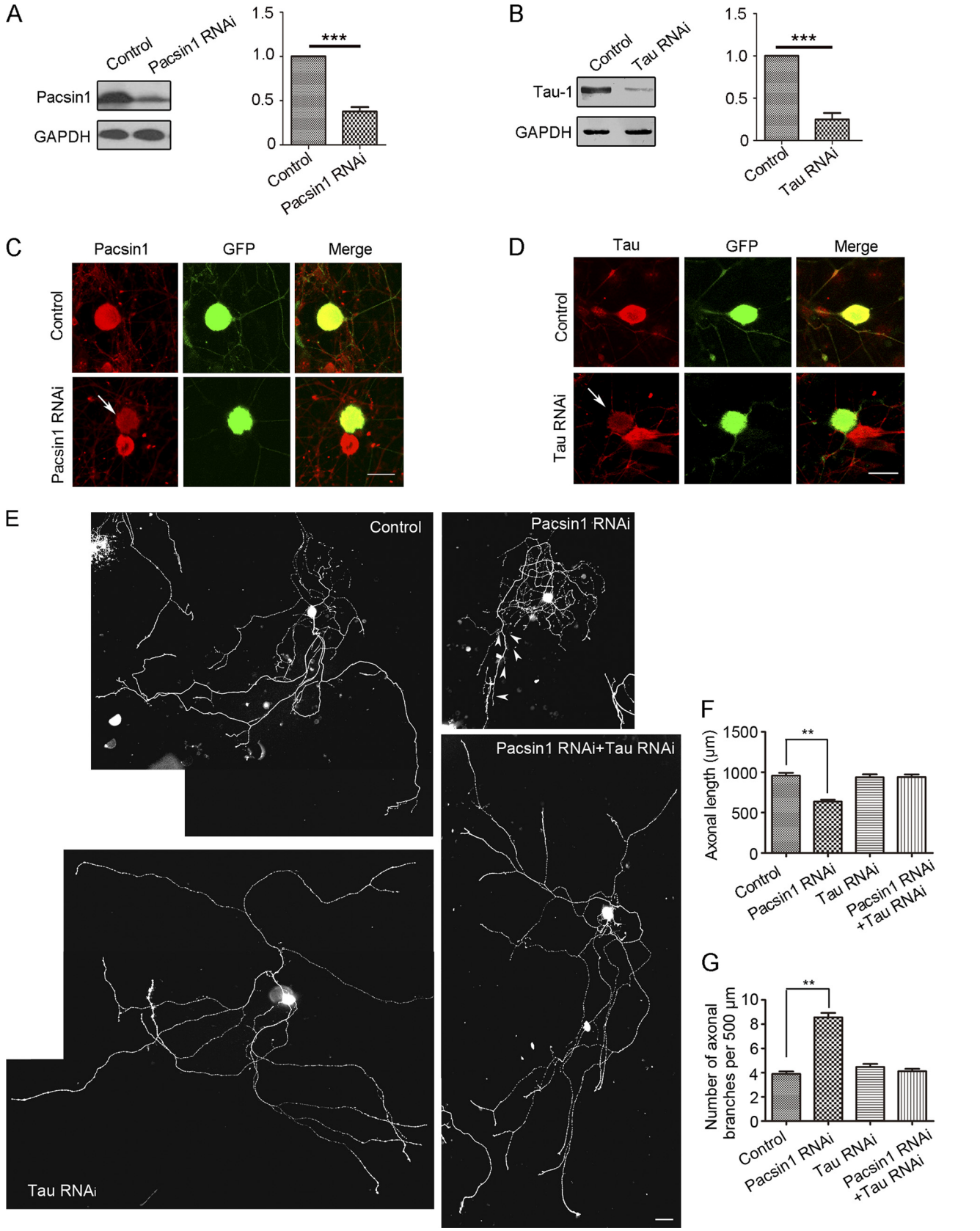

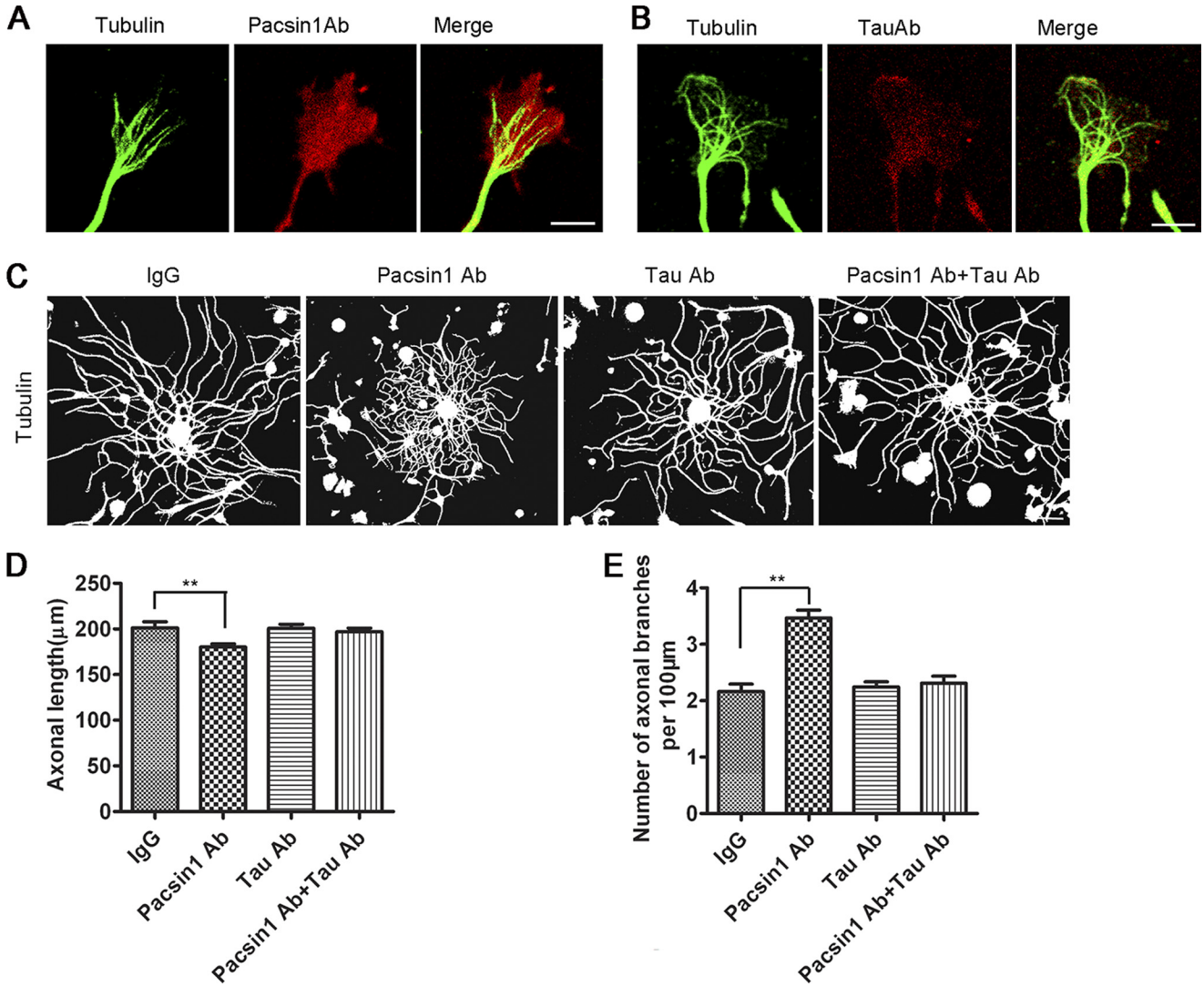

FIGURE 4. **PACSIN1 modulates axonal elongation and branching via Tau, examined by antibody injection.** *A* and *B,* effect of antibodies injected into DRG neurons. DRG neurons were injected with rabbit PACSIN1 Ab (*A*) or rabbit Tau Ab (*B*) and fixed at 1 DIV. The injected neurons exhibited an obvious PACSIN1 (*A, middle panel*) or Tau (*B, middle panel*) distribution pattern, although they were not immunostained with PACSIN1 or Tau primary antibody, indicating that the injected antibodies reacted with the proteins. Injected neurons were also immunostained with anti-tubulin antibody (*left panels*). *Scale bar,* 5 μm. *C,* representative images of DRG neurons stained with anti-α-tubulin antibody at 1 DIV. DRG neurons were injected with IgG, PACSIN1 Ab, Tau Ab, or PACSIN1 Ab+Tau Ab. *Scale bar*, 50 μm. *D* and *E,* quantitative measurement of axonal length (*D*) and number of primary branches (>10 μm, tubulin-positive) (*E*). Blocking of PACSIN1 results in shorter length and higher number of branches. IgG, $n = 68$ axons; PACSIN1 Ab, $n = 104$ axons; Tau Ab, $n = 108$ axons; PACSIN1 Ab+Tau Ab, $n = 104$ axons. One-way analysis of variance, post hoc test, mean ± S.E. **, $p < 0.01$.

Interaction between PACSIN1 and Tau Regulates Neuronal Microtubule Organization—To investigate the cellular mechanism underlying the phenotypes, the microtubule dynamics of GCs were examined. RNAi experiments need 3 days for protein knockdown. However, the GCs of DRG neurons at 3 DIV are too small for further investigation. Next antibody injection was used, because GCs were extended and easy to observe at 1 DIV. First microtubule dynamics was observed by GFP-tagged tubulin in GCs of DRG neurons injected with PACSIN1 Ab. Time-lapse confocal microscopy revealed less dynamic microtubules in the GCs of PACSIN1-deficient neurons than in control neurons. Microtubules varied rapidly within the control cells. However, in the PACSIN1-deficient neurons, microtubules appeared more static (supplemental movies 1 and 2). There-

FIGURE 3. **PACSIN1 regulates axonal elongation and branching through Tau by RNA interference analysis.** *A–D,* knockdown effects of RNA interference constructs targeting PACSIN1 and Tau, respectively. *A* and *B,* HEK293T cells were transfected with pEGFP-PACSIN1+pSuper-PACSIN1 or pEGFP-TauL4+pSuper-Tau. Empty pSuper vector was used as control. Note that PACSIN1 and Tau expression was reduced by 70 and 80%, respectively, 72 h after transfection with RNA interference constructs. Anti-GAPDH antibody is used as loading control. ***, $p < 0.001$. *C–D,* DRG neurons were injected with pEGFP-C1+pSuper-PACSIN1 (*C*), pEGFP-C1+pSuper-Tau (*D*). 72 h later, endogenous PACSIN1 and Tau were examined by immunofluorescence. pSuper vector was used as control. *Left panels* show PACSIN1 (*C*) or Tau (*D*) expression. GFP indicates injected neurons. *Right panels* show merged images. Note that the immunofluorescence density of PACSIN1 and Tau significantly decreased after RNA interference (*arrows*). *Scale bar,* 20 μm. *E,* representative images of DRG neurons at 3 DIV injected with pEGFP+pSuper, pEGFP+pSuper-PACSIN1, pEGFP+pSuper-Tau or pEGFP+pSuper-PACSIN1+pSuper-Tau. Note shorter axonal length and higher number of branches (*arrowheads*) after PACSIN1 knockdown. *Scale bar,* 100 μm. *F* and *G,* quantification of axonal length (*F*) and number of primary branches (*G*) of injected DRG neurons. Control, $n = 134$ axons; PACSIN1 RNAi, $n = 205$ axons; Tau RNAi $n = 108$ axons; PACSIN1 RNAi+Tau RNAi, 141 axons. One-way analysis of variance, post-hoc test, Mean ± S.E. **, $p < 0.01$.

fore, PACSIN1 was thought to reversely correlate with local microtubule stability. In addition, brighter microtubule fluorescence was observed in the shaft of PACSIN1 blocked neurons (data not shown), and thus microtubule density was examined by electron microscopy. Electron microscopic analysis of longitudinal- and cross-sections of axonal shafts from

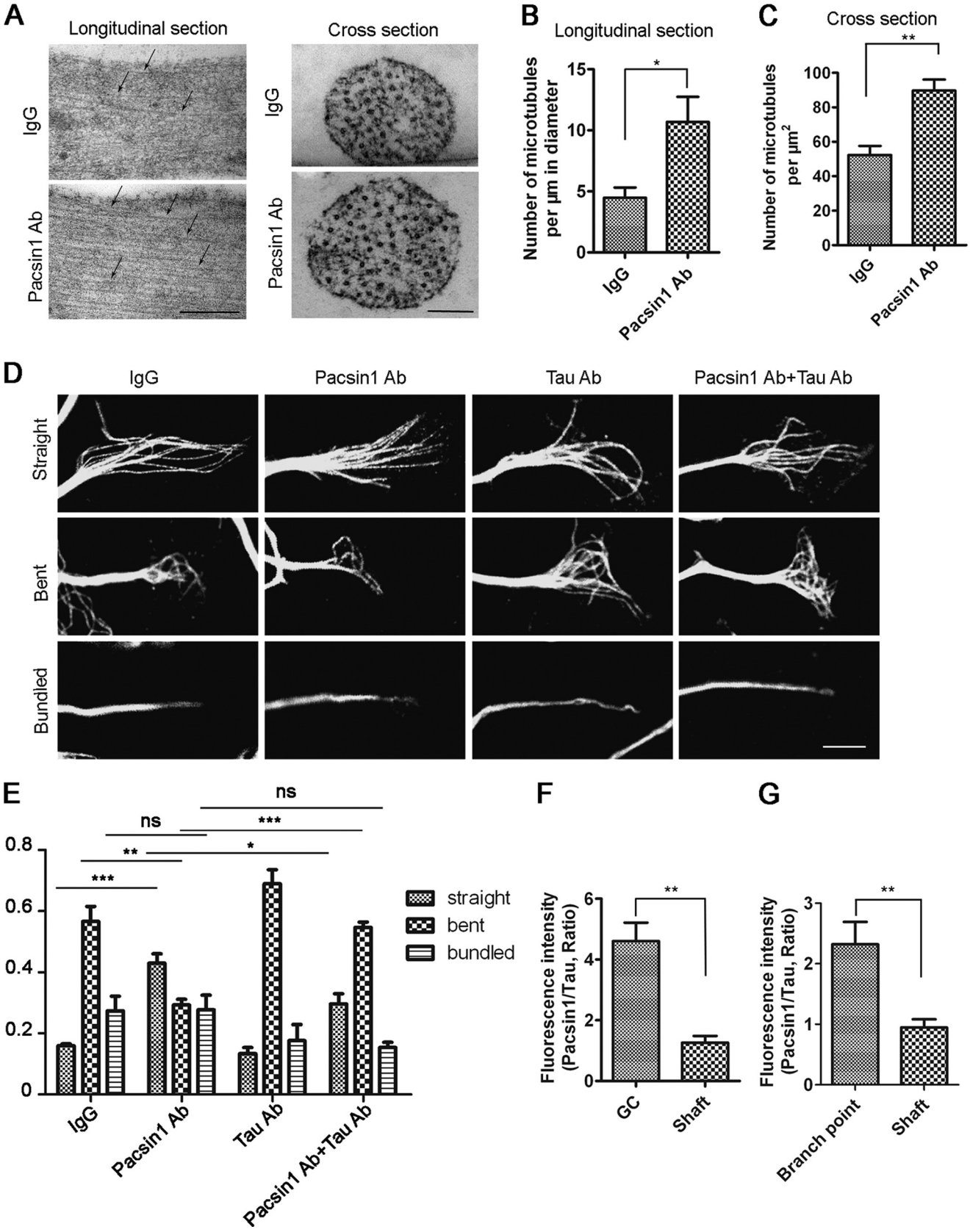

PACSIN1-deficient DRG neurons further revealed greater microtubule density than in control neurons (Fig. 5, *A–C*). These results suggested that PACSIN1 increased microtubule instability.

To examine whether the altered microtubule dynamics observed in PACSIN1-deficient neurons was mediated through Tau, GC microtubule organization of antibody-injected DRG neurons was analyzed. For quantification, the microtubule organization was classified into three type as follows: straight/spread, bent/looped, or bundled (Fig. 5*D*) (31). When PACSIN1 was blocked, a greater number of GCs exhibited straight/spread microtubules (increased to 43%), and fewer GCs exhibited bent/looped microtubules (decreased to 29%) compared with those in control neurons injected with IgG (straight/spread, 16%; bent/looped, 55%) (Fig. 5, *D* and *E*). These results confirmed that PACSIN1 negatively regulates microtubule stability. In addition, the percentage of straight/spread type was reduced, although there were more bent/looped types in PACSIN1/Tau double-blocked (straight/spread, 30%; bent/looped, 55%) than in PACSIN1 single-blocked neurons (straight/spread, 43%; bent/looped, 29%) (Fig. 5, *D* and *E*). The difference between PACSIN1-blocked and control neurons was larger than that between Tau-blocked and PACSIN1/Tau double-blocked neurons. Taken together, PACSIN1 negatively regulates GC microtubule stability by associating with Tau. Consistent with these results, the ratios of PACSIN1 fluorescence intensity to Tau revealed 3- and 1.5-fold more pascin1 than Tau in axonal GCs and branch points where microtubules were not tightly bundled, respectively. However, the pascin1 level was equal to Tau in the shaft with relatively tightly bundled microtubules (Fig. 5, *F* and *G*).

Interaction between PACSIN1 and Tau Is Sufficient for Attenuating Tau-induced Microtubule Polymerization/Stability/Bundling—HeLa cells, which did not endogenously express Tau or PACSIN1, were utilized to further explore microtubule organizational changes caused by their interaction. Microtubule organization between Tau/PACSIN1 and Tau/PACSIN1P434L (no binding ability to Tau) co-expressing cells was compared to reveal Tau-dependent PACSIN1 effects on microtubule stability. First, microtubule repolymerization was performed to determine whether PACSIN1 affected the ability of Tau to promote microtubule assembly in Tau, Tau/PACSIN1, or Tau/PACSIN1P434L-expressing HeLa cells (Fig. 6*A*). Microtubules were depolymerized following cold treatment in all cells, including Tau-expressed cells. After 0.5 min of recovery, microtubules in Tau-expressed cells rapidly repolymerized and were nucleated in many cytoplasmic regions. After 5 min, the microtubules formed tight bundles. In cells co-expressing Tau and PACSIN1P434L, a similar phenomenon was observed (Fig. 6*A*, *right panels*). However, in Tau/PACSIN1 co-expressed cells, no obvious microtubule reassembly was observed at 0.5 min (Fig. 6*A*, *middle panels*). Although the microtubule network began to recover 5 min later, it did not form highly bundled microtubules, but rather it extended microtubules from an organized center (Fig. 6*A*, *middle panels*). In the Tau/PACSIN1 co-expressed cells, fluorescence intensity of repolymerized microtubules was significantly less than in Tau/PACSIN1P434L co-expressed cells after 5 min of re-growth (Fig. 6, *A* and *B*). Therefore, the interaction between PACSIN1 and Tau suppressed Tau-promoting microtubule repolymerization.

Subsequently, the effect of PACSIN1 and Tau on microtubule stability was analyzed. After nocodazole treatment, most RFP-, RFP-PACSIN1-, or RFP-PACSIN1P434L-expressing cells exhibited totally disrupted microtubules (data not shown). However, >90% Tau-expressing cells maintained well polymerized microtubules. As anticipated, the percentage of cells with polymerized microtubules significantly decreased from 60% in Tau/PACSIN1P434L co-expressed cells to 13% in Tau/PACSIN1 co-expressed cells (Fig. 6, *C* and *D*). These results demonstrated an interaction between PACSIN1 and Tau, which reduced nocodazole resistance of microtubules and suggested decreased microtubule stability in the presence of PACSIN1.

Next, the effects of PACSIN1 and Tau interaction on microtubule bundling were analyzed (Fig. 6*E*). For quantification, the microtubule network of transfected cells was classified into three types as follows: tightly, loosely, and slightly bundled (Fig. 6*F*). Approximately 90% of Tau-positive cells exhibited tightly bundled microtubules. Only 20% of Tau/PACSIN1 co-expressed cells exhibited tightly bundled microtubules, whereas 40% of Tau/PACSIN1P434L co-expressed cells did (Fig. 6*G*). Microtubules were more bundled in the presence of PACSIN1P434L than PACSIN1 in Tau-positive cells, which demonstrated that PACSIN1 and Tau interaction reduced the microtubule bundling ability of Tau.

Blocking of PACSIN1 Alters Tau Distribution—To analyze how their interaction affected microtubule dynamics, Tau distribution in PACSIN1-blocked DRG neurons was examined. Tau fluorescence was significantly brighter in the axonal shaft, but weaker in GCs of PACSIN1 Ab-injected neurons than controls (Fig. 7, *A–C*). To eliminate fluorescence intensity differences due to different neurons, the ratio of Tau fluorescence intensity was calculated in the shaft to GC of the same neuron. The ratio in PACSIN1 Ab-microinjected neurons (ratio = 7.5) was significantly greater than in IgG-microinjected neurons (ratio = 4.0) (Fig. 7*D*). The results demonstrated that blocking of PACSIN1 function resulted in increased Tau levels in the shaft, which could increase microtubule stability and contrib-

FIGURE 5. **Regulation of microtubule organization by PACSIN1 and Tau.** *A,* electron micrographs of microtubules (*arrows*) in longitudinal (*left panels*) and cross-sections (*right panels*) of axonal shafts from DRG neurons injected with IgG (*upper panels*) or PACSIN1 Ab (*bottom panels*). *Scale bars,* 250 nm. *B* and *C,* quantification of microtubule density of longitudinal (*B*) and cross-sections (*C*). Note increased density of microtubules in PACSIN1-deficient neurons. *B,* IgG, $n = 5$ axons; PACSIN1 Ab, $n = 5$ axons. *C,* IgG, $n = 13$ axons; PACSIN1 Ab, $n = 25$ axons. Independent samples *t* test; mean ± S.E.; two-tailed. **, $p < 0.01$; *, $p < 0.05$. *D,* examples of different types of microtubule organization in GCs of DRG neurons injected with antibodies as follows: straight/spread (*top panels*), bent/loop (*middle panels*), or bundled (*bottom panels*). *Scale bars,* 5 μm. *E,* histograms of percentage of different types of microtubule organization in GCs of neurons injected with antibodies. Note the percentage of straight microtubules in neurons injected with PACSIN1 Ab increases compared with control. IgG, $n = 245$ GCs; PACSIN1 Ab, $n = 249$ GCs; Tau Ab, $n = 262$ GCs; PACSIN1 Ab+Tau Ab, $n = 318$ GCs. *F* and *G,* ratios of fluorescence intensity of PACSIN1 to Tau. Note that the ratios in GCs and branch points are significantly greater than in the shaft. $n = 13$ axons. Independent samples *t* test. Mean ± S.E. Two-tailed. *, $p < 0.05$; **, $p < 0.01$. *n.s.,* not significant.

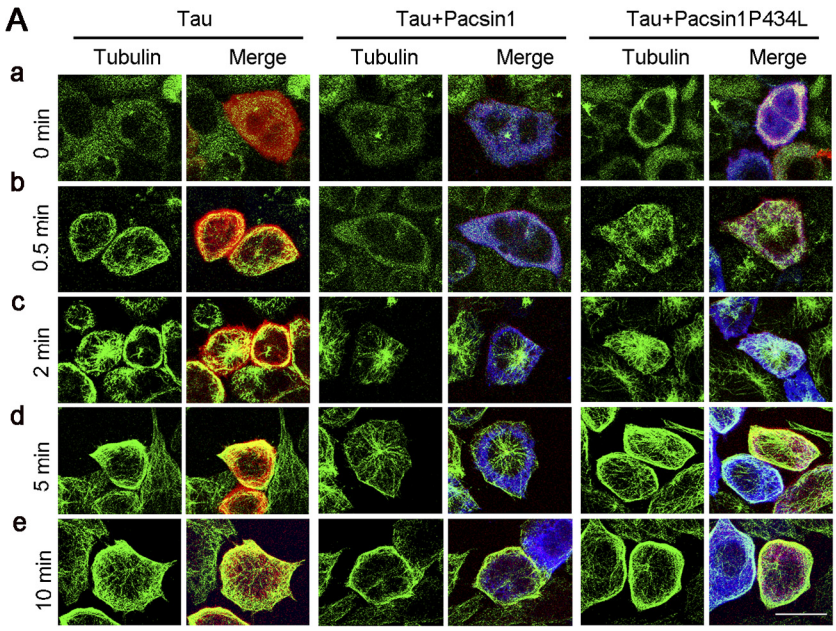

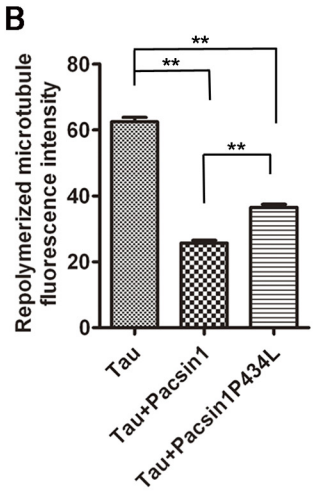

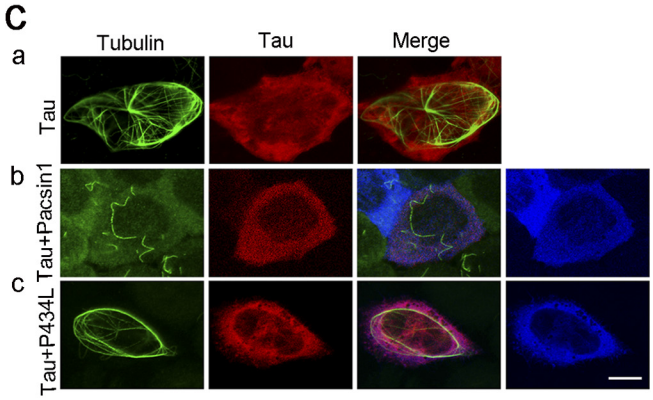

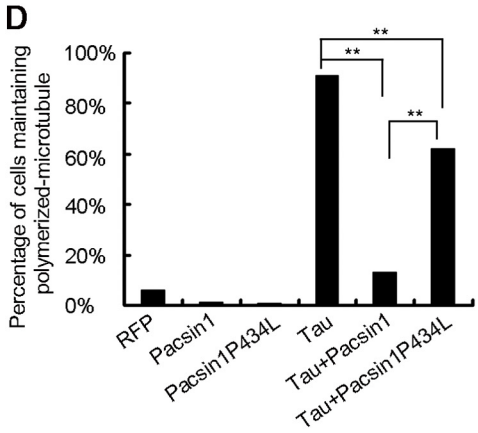

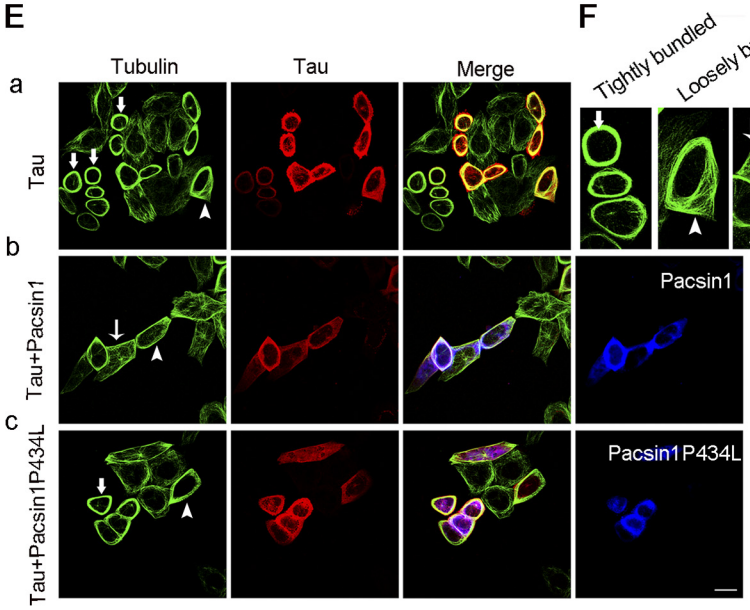

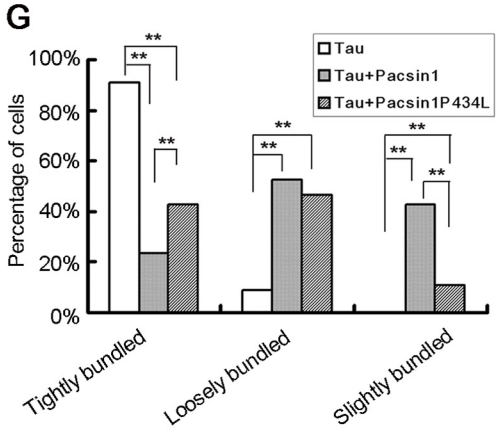

ute to increased microtubule density in the shaft of PACSIN1-blocked neurons (Fig. 5, *A–C*).

The GC is composed of central (C domain) and peripheral (P domain) domains. Microtubules are bundled together in the C domain, and individual microtubules invade the P domain, which is abundant in actin filaments (33). Examination of Tau distribution in the different GC domains of PACSIN1-deficient neurons revealed brighter Tau fluorescence in the C domain but weaker Tau fluorescence in the P domain (Fig. 7, *A*, *B, E,* and *F*). The ratio of the C to P domain in PACSIN1-blocked neurons was significantly greater than in control neurons (Fig. 7*G*), indicating a greater amount of accumulated Tau in the C domain after PACSIN1 blocking. Therefore, PACSIN1 blocking resulted in increased Tau accumulation in the shaft and C domain where microtubules were more bundled and stable.

To confirm that PACSIN1 affected Tau distribution, the *in vitro* tubulin assembly assay was performed in mouse brain homogenates. In the presence of PACSIN1 Ab, a greater amount of Tau and assembled microtubules were in the pellet compared with IgG (Fig. 7, *H–J*), indicating that a greater amount of Tau bound to the microtubules to promote microtubule assembly and formation of a greater mass of stable microtubules. These results confirmed that the absence of PACSIN1 changes Tau distribution to facilitate stable microtubule formation (Fig. 7, *A–G*).

DISCUSSION

This study demonstrated, for the first time, that PACSIN1 plays a crucial role in the regulation of axonal microtubule dynamics via a Tau-mediated mechanism. PACSIN1 was shown to act as a direct binding partner of Tau by pulldown, yeast two-hybrid, and co-immunoprecipitation assays. They exhibited discontinuous distributions and were partially co-localized in neuronal axons. PACSIN1 decreased microtubule stability by reducing the binding ability of Tau to microtubules. Therefore, disrupted interaction between PACSIN1 and Tau suppressed axonal elongation and promoted axonal branching.

New Function of PACSIN1 via Tau Binding—PACSIN1 has been shown to interact with DYNAMIN I, EHD proteins, and other vesicle-related proteins, as well as to participate in endocytosis and vesicle recycling (18, 19, 21). It also interacts with N-WASP and regulates actin organization (22). Via the F-BAR domain, PACSIN1 functions in membrane constriction and tubulation and shapes axonal plasma membrane (24, 25, 34). Interestingly, the present results demonstrate that PACSIN1, by interacting with Tau, modulates axonal microtubule dynamics. This new function of PACSIN1 takes place via a Tau-based mechanism. First, blocking of Tau diminishes the difference in GC microtubule organization between PACSIN1-blocked and control neurons. Second, blocking of Tau abrogates the effects of PACSIN1 on axonal elongation and branching. Third, disruption of the interaction between PACSIN1 and Tau via PACSIN1P434L, a mutant that lacks Tau binding, significantly attenuates the effects of PACSIN1 on microtubule organization. Therefore, Tau binding allows PACSIN1 to regulate axonal microtubule dynamics.

In this study, we showed that altered Tau distribution following PACSIN1 RNAi led to the formation of straighter microtubules, which resulted in neurons with a shorter axonal length and higher number of branch points (Fig. 3, *E–G*). It remains to be further studied whether overexpression of PACSIN1 could play an opposite role in axonal length and branch points through reducing the microtubule bundling ability of Tau.

Organization of GC Microtubules—Tau co-localizes with microtubules and is abundant in GCs, especially in the microtubule-rich C domain (30). In GCs, Tau assembles tubulin and bundles dynamic microtubules into well organized microtubules (11). Although microtubule organization does not significantly change in GCs of $tau^{-/-}$ mice because of a functional redundancy of MAP1A, abnormalities in GC cytoskeletal organization are observed in $tau^{-/-}map1b^{-/-}$ mice (10, 11). The C domain of $tau^{-/-}map1b^{-/-}$ neurons extends with little bundled microtubules, which resulted in defective axonal elongation. Interestingly, PACSIN1 is significantly more abundant than Tau in GCs and branch points where microtubules are relatively unstable, which suggests that PACSIN1 spatially restricts the effect of Tau on promoting microtubule stability. In PACSIN1-blocked DRG neurons, Tau fluorescence intensity increased in the shaft and C domains, which suggests that a greater amount of Tau was localized in organized parallel arrays of axonal microtubules following PACSIN1 blocking. Indeed, a greater number of straight GC microtubules and a greater density of microtubules in PACSIN1-blocked neurons were

FIGURE 6. **PACSIN1 suppresses Tau-induced microtubule repolymerization, stability, and bundling.** *A* and *B,* PACSIN1 suppresses Tau-induced microtubule repolymerization. *A,* representative examples of microtubule (*green*) repolymerization at different time points after cold treatment. Merged images are as follows: *green,* tubulin; *red,* RFP-Tau; *blue,* Myc-PACSIN1 or PACSIN1P434L. HeLa cells expressing RFP-Tau (*left panels*), RFP-Tau+Myc-PACSIN1 (*middle panels*), or RFP-Tau+Myc-PACSIN1P434L (*right panels*) were treated on ice for 2 h and immunostained with anti-α-tubulin and anti-PACSIN1 antibodies to examine microtubule repolymerization at 37 °C at different time points. Note that microtubule repolymerization is retarded in the presence of PACSIN1. *Scale bar,* 20 μm. *B,* fluorescence intensity of repolymerized microtubules in RFP-Tau ($n = 290$)-, RFP-Tau+Myc-PACSIN1 ($n = 123$)-, or RFP-Tau+Myc-PACSIN1P434L ($n = 212$)-transfected cells after rewarming for 5 min. Note significant reduction in the presence of PACSIN1. One-way analysis of variance, post hoc test, means ± S.E. **, $p < 0.01$. *C* and *D,* interaction between PACSIN1 and Tau reduces microtubule stability promoted by Tau. *C,* immunostaining of microtubules (*green*) in transfected HeLa cells after treatment with nocodazole (10 μg/ml) for 1.5 h. *Red*, RFP-Tau; *blue,* Myc-PACSIN1 or PACSIN1P434L. The resistance of microtubules to depolymerization induced by nocodazole is reduced in RFP-Tau+Myc-PACSIN1 cells (*C, panel b*), compared with RFP-Tau (*C, panel a*) and RFP-Tau+Myc-PACSIN1P434L cells (*C, panel c*). *Scale bar,* 10 μm. *D,* quantification of cells maintaining polymerized microtubules after nocodazole treatment. Polymerized microtubules are observed in >60% of Tau+PACSIN1P434L co-expressed cells, but only in 13% of Tau+PACSIN1 co-expressed cells. *RFP*, $n = 82$; *pacsin1*, $n = 140$; *pacsin1P434L*, $n = 106$; *tau*, $n = 90$; *tau+pacsin1*, $n = 54$; *tau+pacsin1P434L*, $n = 89$. Hundred percent testing. **, $p < 0.01$. *E–G,* interaction of PACSIN1 and Tau reduces Tau-induced microtubule bundling. *E,* immunostaining of microtubules (*green*) in transfected HeLa cells. *Red,* RFP-Tau; *blue,* Myc-PACSIN1 or PACSIN1P434L. *F,* magnified images of cells show three types of microtubule organization. *Thick arrows, arrowheads*, and *thin arrows* indicate tightly bundled, loosely bundled, and slightly bundled microtubules, respectively. Microtubules in RFP-Tau+Myc-PACSIN1-expressing HeLa cells (*E, panel b*) are less bundled than RFP-Tau (*E, panel a*)- and RFP-Tau+Myc-PACSIN1P434L (*E, panel c*)-expressing cells. *Scale bars,* 20 μm. *G,* quantification data of *E*. The percentage of cells possessing tightly bundled microtubules are significantly less in the presence of PACSIN1 compared with PACSIN1P434L. However, characteristics of slightly bundled microtubules are opposite. *Tau*, $n = 448$; *tau+pacsin1*, $n = 232$; *tau+pacsin1P434L*, $n = 258$. Hundred percent testing. **, $p < 0.01$.

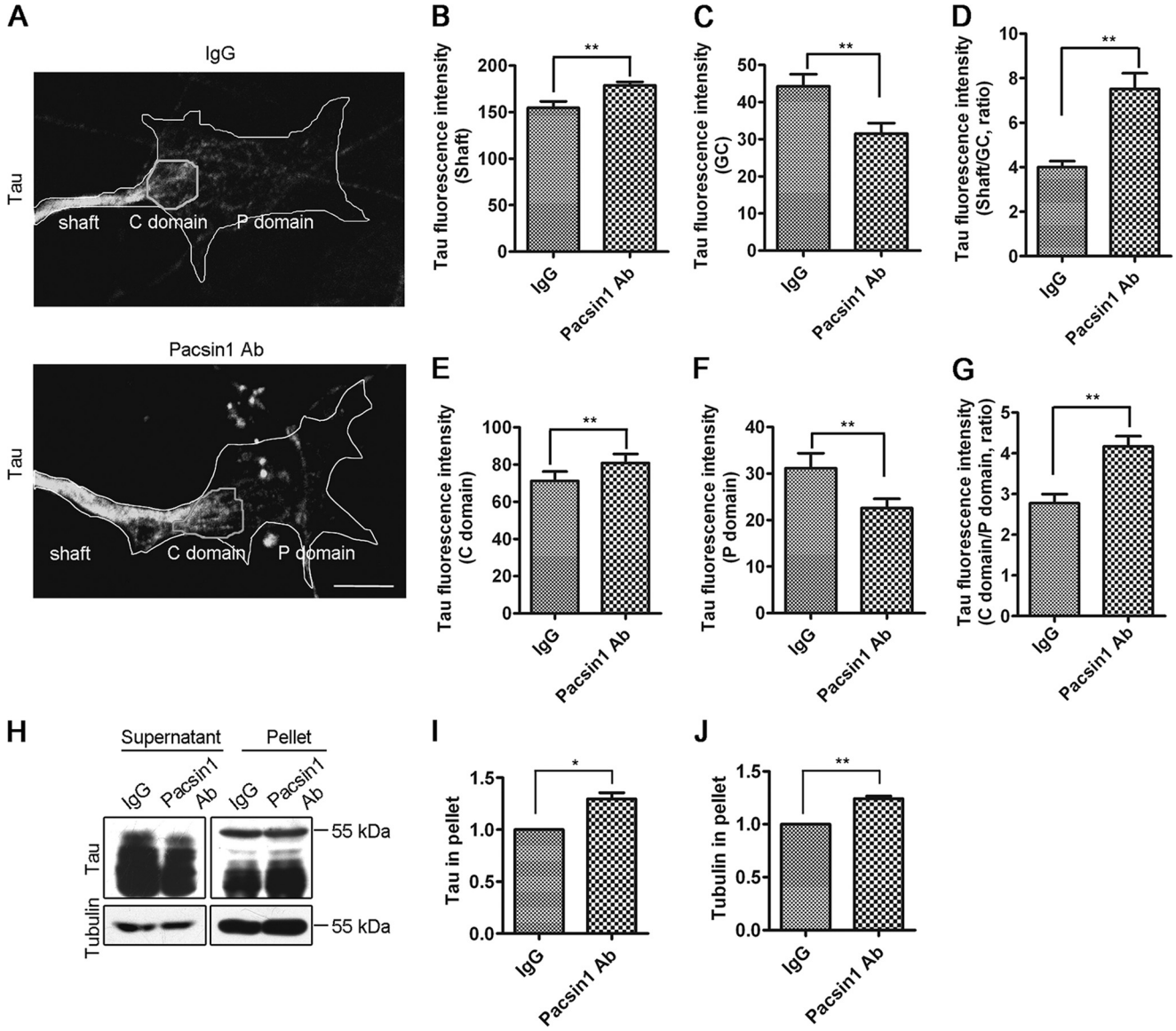

FIGURE 7. **Blocking of PACSIN1 induces changes in Tau distribution.** *A,* representative fluorescent images of Tau in GCs of DRG neurons injected with IgG (*upper panel*) or PACSIN1 Ab (*bottom panel*). The edge of GCs is *outlined*. *Scale bar*, 5 μm. *B, C, E,* and *F,* Tau fluorescence intensity in shaft (*B*), GC (*C*), C domain (*E*), and P domain (*F*). *D* and *G,* ratios of Tau fluorescence intensity in shaft to GC (*D*) and C domain to P domain (*G*). Note that these two ratios in neurons injected with PACSIN1 Ab are significantly greater than neurons injected with IgG. IgG, $n = 38$ axons; PACSIN1 Ab, $n = 41$ axons. Independent samples *t* test, mean $\pm$ S.E., two-tailed. **, $p < 0.01$. *H,* Tau and α-tubulin in supernatants and pellets, when microtubules are assembled from tubulins in mouse brain lysates in the presence of IgG or PACSIN1 Ab. *I* and *J,* quantitative analysis of Tau and tubulin bands. Normalized to IgG in percentage. Note that more Tau and tubulin appears in pellet in the presence of PACSIN1 Ab. $n = 3$. Independent sample *t* test, mean $\pm$ S.E., two-tailed. **, $p < 0.01$; *, $p < 0.05$.

observed. Our biochemical results also show that Tau binding to microtubules is impaired in the presence of PACSIN1. These results indicate that PACSIN1 negatively regulates microtubule stability by decreasing Tau binding to microtubules.

Axonal Morphogenesis—At axonal branch sites, microtubules become unbundled and undergo fragmentation; the short microtubules then invade filopodial processes with forward, backward, and lateral movements (35–38). Microtubule invasion is necessary for branch formation, although it does not guarantee branch survival (38). Therefore, consolidation of the microtubule invasion by more stable microtubules is crucial for branching. PACSIN1 was enriched in branch points, suggesting its role in axonal branching. In PACSIN1 Ab-injected neurons, a greater amount of Tau resulted in the formation of more stable microtubules and the promotion of branch outgrowth. This was similar to previous reports that CRMP-2 (a microtubule stabilizer) overexpression promotes axonal branching (3), prevention of the microtubule destabilizing activity of SCLIP (SCG-10 like protein) increases axonal branching (39), and loss of KIF2A (a microtubule destabilizer) extends more collateral branches (40).

Reorganization of the microtubule cytoskeleton in response to external stimuli and internal cues largely affects axonal growth (3, 41), and control of microtubule dynamics by various factors, including MAP, is crucial to this process (1, 3, 4). Either decreasing (11) or increasing expression (3, 41) of MAPs impairs normal axonal elongation. In addition, taxol and nocodazole treatment disrupt the balance between stable and

dynamic microtubules, which results in axonal growth inhibition (4). PACSIN1 could function as a molecular switch between stable and dynamic microtubules by modulating Tau binding to microtubules. When PACSIN1 was blocked in this study, the microtubules were significantly more stable because of increased Tau binding, which subsequently impaired axonal elongation. Also, formation of more branches in PACSIN1-blocked neurons, which needed a greater number of microtubules redistributing into these branches, resulted in a decreased elongation of the primary axon (41). However, knockdown of PACSIN1 in hippocampal neurons promotes axonal growth (25). It is not certain whether the difference is caused by different kinds of neurons or a different degree of PACSIN1 blocking.

Role of PACSIN1 in Microtubules and Actin Filaments—Cross-talk between microtubules and actin filaments is thought to be required during axonal development (42, 43). PACSIN1 has been shown to interact with N-WASP, which is associated with actin polymerization (21), and this interaction affects neuronal morphology (25). This study suggests that PACSIN1 function in neuronal morphogenesis requires Tau-related microtubule dynamics. Therefore, it is likely that PACSIN1 influences neuronal morphology via two parallel pathways, via a Tau-mediated microtubule network and N-WASP-regulated actin filaments. In fact, following permeabilization, with exception to co-localization with Tau and function in Tau-related microtubule dynamics, PACSIN1 exists at the cell periphery where actin filaments are abundant and could participate in multiple cellular events, including actin-related process.

In summary, results from this study provide strong evidence that PACSIN1 acts as a negative regulator in microtubule stability by binding directly to Tau. This interaction could modulate microtubule dynamics in a spatial and temporal manner to ensure proper axonal morphogenesis. Defects in microtubule organization have been linked to many nervous system disorders (44). In fact, PACSIN1 plays a critical role during the early stage of Huntington disease (45), and Tau has been correlated with Alzheimer disease (15). Further studies are needed, however, to determine whether aberrant regulation of this interaction leads to neurodegenerative disease.

Acknowledgments—We are grateful to Dr. M. Plomann (University of Cologne, Germany) for PACSIN1 cDNA. We thank X. L. Su (Harvard University), Q. Wang (Peking University), and Y. Wang (Pennsylvania University) for editing and critical reading of the manuscript.

REFERENCES

1. Buck, K. B., and Zheng, J. Q. (2002) Growth cone turning induced by direct local modification of microtubule dynamics. *J. Neurosci.* **22,** 9358–9367
2. Inagaki, N., Chihara, K., Arimura, N., Ménager, C., Kawano, Y., Matsuo, N., Nishimura, T., Amano, M., and Kaibuchi, K. (2001) CRMP-2 induces axons in cultured hippocampal neurons. *Nat. Neurosci.* **4,** 781–782
3. Fukata, Y., Itoh, T. J., Kimura, T., Ménager, C., Nishimura, T., Shiromizu, T., Watanabe, H., Inagaki, N., Iwamatsu, A., Hotani, H., and Kaibuchi, K. (2002) CRMP-2 binds to tubulin heterodimers to promote microtubule assembly. *Nat. Cell Biol.* **4,** 583–591
4. Witte, H., Neukirchen, D., and Bradke, F. (2008) Microtubule stabilization specifies initial neuronal polarization. *J. Cell Biol.* **180,** 619–632
5. Goedert, M., Crowther, R. A., and Garner, C. C. (1991) Molecular characterization of microtubule-associated proteins Tau and MAP2. *Trends Neurosci.* **14,** 193–199
6. Hirokawa, N. (1994) Microtubule organization and dynamics dependent on microtubule-associated proteins. *Curr. Opin. Cell Biol.* **6,** 74–81
7. Chen, J., Kanai, Y., Cowan, N. J., and Hirokawa, N. (1992) Projection domains of MAP2 and Tau determine spacings between microtubules in dendrites and axons. *Nature* **360,** 674–677
8. Drubin, D. G., and Kirschner, M. W. (1986) Tau protein function in living cells. *J. Cell Biol.* **103,** 2739–2746
9. Kanai, Y., Takemura, R., Oshima, T., Mori, H., Ihara, Y., Yanagisawa, M., Masaki, T., and Hirokawa, N. (1989) Expression of multiple Tau isoforms and microtubule bundle formation in fibroblasts transfected with a single Tau cDNA. *J. Cell Biol.* **109,** 1173–1184
10. Harada, A., Oguchi, K., Okabe, S., Kuno, J., Terada, S., Ohshima, T., Sato-Yoshitake, R., Takei, Y., Noda, T., and Hirokawa, N. (1994) Altered microtubule organization in small-caliber axons of mice lacking Tau protein. *Nature* **369,** 488–491
11. Takei, Y., Teng, J., Harada, A., and Hirokawa, N. (2000) Defects in axonal elongation and neuronal migration in mice with disrupted *tau* and *map1b* genes. *J. Cell Biol.* **150,** 989–1000
12. Wagner, U., Utton, M., Gallo, J. M., and Miller, C. C. (1996) Cellular phosphorylation of Tau by GSK-3β influences Tau binding to microtubules and microtubule organization. *J. Cell Sci.* **109,** 1537–1543
13. Biernat, J., Wu, Y. Z., Timm, T., Zheng-Fischhöfer, Q., Mandelkow, E., Meijer, L., and Mandelkow, E. M. (2002) Protein kinase MARK/PAR-1 is required for neurite outgrowth and establishment of neuronal polarity. *Mol. Biol. Cell* **13,** 4013–4028
14. Sang, H., Lu, Z., Li, Y., Ru, B., Wang, W., and Chen, J. (2001) Phosphorylation of Tau by glycogen synthase kinase 3β in intact mammalian cells influences the stability of microtubules. *Neurosci. Lett.* **312,** 141–144
15. Sergeant, N., Delacourte, A., and Buée, L. (2005) Tau protein as a differential biomarker of tauopathies. *Biochim. Biophys. Acta* **1739,** 179–197
16. Plomann, M., Lange, R., Vopper, G., Cremer, H., Heinlein, U. A., Scheff, S., Baldwin, S. A., Leitges, M., Cramer, M., Paulsson, M., and Barthels, D. (1998) PACSIN, a brain protein that is up-regulated upon differentiation into neuronal cells. *Eur. J. Biochem.* **256,** 201–211
17. Kessels, M. M., and Qualmann, B. (2002) Syndapins integrate N-WASP in receptor-mediated endocytosis. *EMBO J.* **21,** 6083–6094
18. Modregger, J., Ritter, B., Witter, B., Paulsson, M., and Plomann, M. (2000) All three PACSIN isoforms bind to endocytic proteins and inhibit endocytosis. *J. Cell Sci.* **113,** 4511–4521
19. Braun, A., Pinyol, R., Dahlhaus, R., Koch, D., Fonarev, P., Grant, B. D., Kessels, M. M., and Qualmann, B. (2005) EHD proteins associate with syndapin I and II and such interactions play a crucial role in endosomal recycling. *Mol. Biol. Cell* **16,** 3642–3658
20. Anggono, V., Smillie, K. J., Graham, M. E., Valova, V. A., Cousin, M. A., and Robinson, P. J. (2006) Syndapin I is the phosphorylation-regulated dynamin I partner in synaptic vesicle endocytosis. *Nat. Neurosci.* **9,** 752–760
21. Qualmann, B., Roos, J., DiGregorio, P. J., and Kelly, R. B. (1999) Syndapin I, a synaptic dynamin-binding protein that associates with the neural Wiskott-Aldrich syndrome protein. *Mol. Biol. Cell* **10,** 501–513
22. Qualmann, B., and Kelly, R. B. (2000) Syndapin isoforms participate in receptor-mediated endocytosis and actin organization. *J. Cell Biol.* **148,** 1047–1062
23. Grimm-Günter, E. M., Milbrandt, M., Merkl, B., Paulsson, M., and Plomann, M. (2008) PACSIN proteins bind tubulin and promote microtubule assembly. *Exp. Cell Res.* **314,** 1991–2003
24. Wang, Q., Navarro, M. V., Peng, G., Molinelli, E., Goh, S. L., Judson, B. L., Rajashankar, K. R., and Sondermann, H. (2009) Molecular mechanism of membrane constriction and tubulation mediated by the F-BAR protein PACSIN/Syndapin. *Proc. Natl. Acad. Sci. U.S.A.* **106,** 12700–12705
25. Dharmalingam, E., Haeckel, A., Pinyol, R., Schwintzer, L., Koch, D., Kessels, M. M., and Qualmann, B. (2009) F-BAR proteins of the syndapin family shape the plasma membrane and are crucial for neuromorphogenesis. *J. Neurosci.* **29,** 13315–13327
26. Kanai, Y., Chen, J., and Hirokawa, N. (1992) Microtubule bundling by Tau proteins *in vivo*. Analysis of functional domains. *EMBO J.* **11,** 3953–3961
27. Clayton, E. L., Anggono, V., Smillie, K. J., Chau, N., Robinson, P. J., and

Cousin, M. A. (2009) The phospho-dependent dynamin-syndapin interaction triggers activity-dependent bulk endocytosis of synaptic vesicles. *J. Neurosci.* **29,** 7706–7717
28. Li, H., Guo, Y., Teng, J., Ding, M., Yu, A. C., and Chen, J. (2006) 14-3-3γ affects dynamics and integrity of glial filaments by binding to phosphorylated GFAP. *J. Cell Sci.* **119,** 4452–4461
29. Okabe, S., and Hirokawa, N. (1990) Turnover of fluorescently labeled tubulin and actin in the axon. *Nature* **343,** 479–482
30. Black, M. M., Slaughter, T., Moshiach, S., Obrocka, M., and Fischer, I. (1996) Tau is enriched on dynamic microtubules in the distal region of growing axons. *J. Neurosci.* **16,** 3601–3619
31. Teng, J., Takei, Y., Harada, A., Nakata, T., Chen, J., and Hirokawa, N. (2001) Synergistic effects of MAP2 and MAP1B knockout in neuronal migration, dendritic outgrowth, and microtubule organization. *J. Cell Biol.* **155,** 65–76
32. Yoshimura, T., Kawano, Y., Arimura, N., Kawabata, S., Kikuchi, A., and Kaibuchi, K. (2005) GSK-3β regulates phosphorylation of CRMP-2 and neuronal polarity. *Cell* **120,** 137–149
33. Rodriguez, O. C., Schaefer, A. W., Mandato, C. A., Forscher, P., Bement, W. M., and Waterman-Storer, C. M. (2003) Conserved microtubule-actin interactions in cell movement and morphogenesis. *Nat. Cell Biol.* **5,** 599–609
34. Rao, Y., Ma, Q., Vahedi-Faridi, A., Sundborger, A., Pechstein, A., Puchkov, D., Luo, L., Shupliakov, O., Saenger, W., and Haucke, V. (2010) Molecular basis for SH3 domain regulation of F-BAR-mediated membrane deformation. *Proc. Natl. Acad. Sci. U.S.A.* **107,** 8213–8218
35. Kornack, D. R., and Giger, R. J. (2005) Probing microtubule + TIPs. Regulation of axon branching. *Curr. Opin. Neurobiol.* **15,** 58–66
36. Yu, W., Ahmad, F. J., and Baas, P. W. (1994) Microtubule fragmentation and partitioning in the axon during collateral branch formation. *J. Neurosci.* **14,** 5872–5884
37. Kalil, K., Szebenyi, G., and Dent, E. W. (2000) Common mechanisms underlying growth cone guidance and axon branching. *J. Neurobiol.* **44,** 145–158
38. Dent, E. W., Callaway, J. L., Szebenyi, G., Baas, P. W., and Kalil, K. (1999) Reorganization and movement of microtubules in axonal growth cones and developing interstitial branches. *J. Neurosci.* **19,** 8894–8908
39. Poulain, F. E., and Sobel, A. (2007) The "SCG10-LIke Protein" SCLIP is a novel regulator of axonal branching in hippocampal neurons, unlike SCG10. *Mol. Cell. Neurosci.* **34,** 137–146
40. Homma, N., Takei, Y., Tanaka, Y., Nakata, T., Terada, S., Kikkawa, M., Noda, Y., and Hirokawa, N. (2003) Kinesin superfamily protein 2A (KIF2A) functions in suppression of collateral branch extension. *Cell* **114,** 229–239
41. Mantych, K. B., and Ferreira, A. (2001) Agrin differentially regulates the rates of axonal and dendritic elongation in cultured hippocampal neurons. *J. Neurosci.* **21,** 6802–6809
42. Dent, E. W., and Kalil, K. (2001) Axon branching requires interactions between dynamic microtubules and actin filaments. *J. Neurosci.* **21,** 9757–9769
43. Witte, H., and Bradke, F. (2008) The role of the cytoskeleton during neuronal polarization. *Curr. Opin. Neurobiol.* **18,** 479–487
44. Tischfield, M. A., Baris, H. N., Wu, C., Rudolph, G., Van Maldergem, L., He, W., Chan, W. M., Andrews, C., Demer, J. L., Robertson, R. L., Mackey, D. A., Ruddle, J. B., Bird, T. D., Gottlob, I., Pieh, C., Traboulsi, E. I., Pomeroy, S. L., Hunter, D. G., Soul, J. S., Newlin, A., Sabol, L. J., Doherty, E. J., de Uzcátegui, C. E., de Uzcátegui, N., Collins, M. L., Sener, E. C., Wabbels, B., Hellebrand, H., Meitinger, T., de Berardinis, T., Magli, A., Schiavi, C., Pastore-Trossello, M., Koc, F., Wong, A. M., Levin, A. V., Geraghty, M. T., Descartes, M., Flaherty, M., Jamieson, R. V., Møller, H. U., Meuthen, I., Callen, D. F., Kerwin, J., Lindsay, S., Meindl, A., Gupta, M. L., Jr., Pellman, D., and Engle, E. C. (2010) Human TUBB3 mutations perturb microtubule dynamics, kinesin interactions, and axon guidance. *Cell* **140,** 74–87
45. Modregger, J., DiProspero, N. A., Charles, V., Tagle, D. A., and Plomann, M. (2002) PACSIN 1 interacts with huntingtin and is absent from synaptic varicosities in presymptomatic Huntington's disease brains. *Hum. Mol. Genet.* **11,** 2547–2558
46. Hughes, G. B., Bottomy, M. B., Jackson, C. G., Glasscock, M. E., 3rd, and Sismanis, A. (1981) Myelin and axon degeneration following direct current peripheral nerve stimulation. A prospective controlled experimental study. *Otolaryngol. Head Neck Surg.* **89,** 767–775

Supplementary Figure 1. Screening of tau-binding proteins. (**A**) Negative control using GST only. 1-5 numbering along the top of each panel means the five samples obtained by sequential elution under the same concentration of NaCl. (**B**) GST-tauL4ΔMBD pull-down adult mouse brain lysates. Pacsin1 in 400 mM NaCl-eluates was visualized by Coomassie brilliant blue staining (arrow).

Supplementary Figure 2. Antibody detection and characterization of pacsin1 expression. (**A**) Immunoblotting of adult mouse brain lysates with self-prepared anti-pacsin1 antibody. Arrow shows the position of pacsin1. (**B**) Immunoblotting of adult mouse brain lysates with self-prepared anti-tau antibody. (**C**) Different tissue lysates of adult mouse were analyzed by Western blotting with rabbit anti-pacsin1 antibody. Pacsin1 is specifically expressed in brain. (**D**) Developmental expression pattern of pacsin1 in mouse brain with rabbit anti-pacsin1 antibody. Expression of pacsin1 increases continuously from E14 to adult age. Anti-tubulin antibody is used as loading control.

Supplementary Figure 3. Immunofluorescent images of cryosections from the adult mouse brain. Green, pacsin1; Red, tau. Top and bottom panels: magnified view of boxed region of middle panels. Pacsin1 and tau co-localized in corpus callosa (arrows, top panels). Note co-localization of pacsin1 and tau in mossy fibers in hippocampal region (arrows, bottom panels). Scale bars, 200 μm.

Supplementary Movie 1. Microtubule dynamics in GFP-tubulin overexpressing DRG neurons injected with IgG. Note that microtubules vary rapidly. Images were captured every 10 seconds.

Supplementary Movie 2. Microtubule dynamics in GFP-tubulin overexpressing DRG neurons injected with pacsin1 Ab. Note that microtubules appear more static. Images were captured every 10 seconds.

Supplementary Figure 1

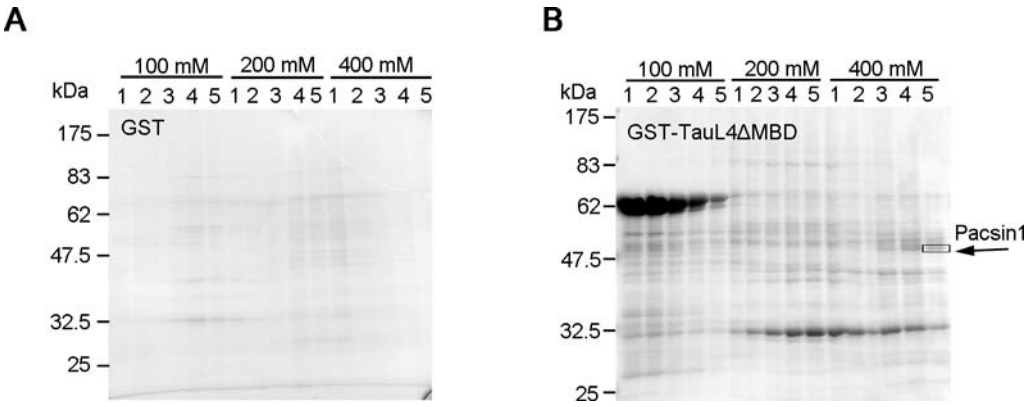

Supplementary Figure 2

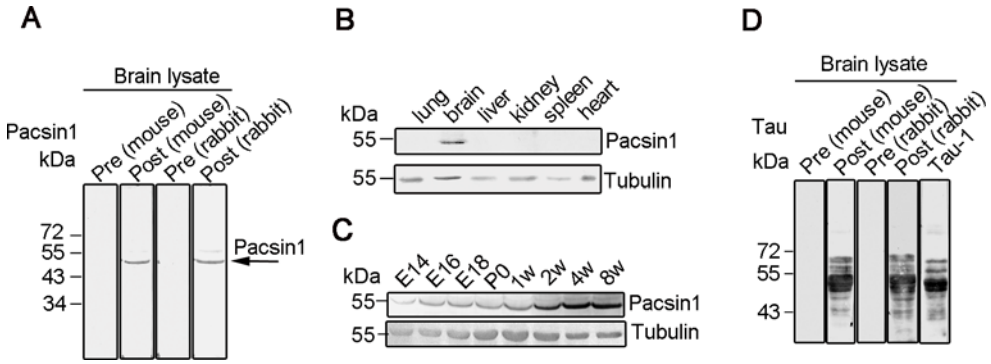

Supplementary Figure 3